NRL Memorandum Report 4111

Theory of the Resistive Hose Instability in Relativistic Electron Beams

HAN S. UHM

Naval Surface Weapons Center
White Oak, Silver Spring, Md. 20910

AND

MARTIN LAMPE

Plasma Theory Branch
Plasma Physics Division

November 26, 1979

Sponsored by
Defense Advanced Research Projects Agency (DoD)
ARPA Order No. 3718
Monitored by C. M. Huddleston Under Contract # N60921-79-WR-W0186

NAVAL RESEARCH LABORATORY
Washington, D.C.

(9) Memorandum rept.,

SECURITY CLASSIFICATION OF THIS PAGE (When Data Entered)

REPORT DOCUMENTATION PAGE	READ INSTRUCTIONS BEFORE COMPLETING FORM
1. REPORT NUMBER: NRL Memorandum Report 4111	2. GOVT ACCESSION NO. / 3. RECIPIENT'S CATALOG NUMBER
4. TITLE (and Subtitle): (6) THEORY OF THE RESISTIVE HOSE INSTABILITY IN RELATIVISTIC ELECTRON BEAMS.	5. TYPE OF REPORT & PERIOD COVERED: Interim report on a continuing NRL problem. / 6. PERFORMING ORG. REPORT NUMBER
7. AUTHOR(s): (10) Han S. Uhm* and Martin Lampe	8. CONTRACT OR GRANT NUMBER(s): (11) 26 Nov 79
9. PERFORMING ORGANIZATION NAME AND ADDRESS: Naval Research Laboratory, Washington, DC 20375 (15) DARPA Order-3718	10. PROGRAM ELEMENT, PROJECT, TASK AREA & WORK UNIT NUMBERS: NRL Problem R08-93B (12) 47
11. CONTROLLING OFFICE NAME AND ADDRESS: Defense Advanced Research Projects Agency, Arlington, VA 22209	12. REPORT DATE: November 26, 1979 / 13. NUMBER OF PAGES: 47
14. MONITORING AGENCY NAME & ADDRESS(if different from Controlling Office): Naval Surface Weapons Center, White Oak, Silver Spring, MD 20910	15. SECURITY CLASS. (of this report): UNCLASSIFIED / 15a. DECLASSIFICATION/DOWNGRADING SCHEDULE

16. DISTRIBUTION STATEMENT (of this Report)

Approved for public release; distribution unlimited.

(14) NRL-MR-4111

17. DISTRIBUTION STATEMENT (of the abstract entered in Block 20, if different from Report)

18. SUPPLEMENTARY NOTES

The views and conclusions contained in this document are those of the authors and should not be interpreted as representing the official policies, either expressed or implied, of the Defense Advanced Research Projects Agency or the U.S. Government.

(Continues)

19. KEY WORDS (Continue on reverse side if necessary and identify by block number)

Hose instability
Beam propagation
Relativistic electron beams
Beam instabilities
Instabilities - linear

(Theta)

20. ABSTRACT (Continue on reverse side if necessary and identify by block number)

A Vlasov-Maxwell theory of the resistive hose instability is developed, for an infinitely long relativistic electron beam propagating parallel to an applied axial magnetic field. Complete space charge neutralization by the ambient plasma, and paraxial flow ($p_z^2 \gg p_r^2 + p_\theta^2$) are assumed. The analysis is performed for rigid-rotor and cold laminar flow equilibria. An integro-differential eigenvalue equation is obtained for the general case, and is reduced to an ordinary differential equation in either the cold laminar flow limit or the case of a square beam density profile. Using

(Continues)

DD FORM 1 JAN 73 1473 EDITION OF 1 NOV 65 IS OBSOLETE
S/N 0102-014-6601

SECURITY CLASSIFICATION OF THIS PAGE (When Data Entered)

251 950

JOB

18. Supplementary Notes (Continued)

This work was sponsored by Defense Advanced Research Projects Agency (DoD) under ARPA Order No. 3718, Amendment No. 2.
*Naval Surface Weapons Center, White Oak, Silver Spring, MD 20910

20. Abstract (Continued)

a variational technique, an approximate dispersion relation is found for arbitrary density profile, and evaluated in closed form for either the Bennett or square profile. Stability properties are illustrated and discussed in detail for a square profile, including the influence of the applied magnetic field (stabilizing), proximity to a conducting guide (stabilizing), and partial current neutralization (destabilizing).

CONTENTS

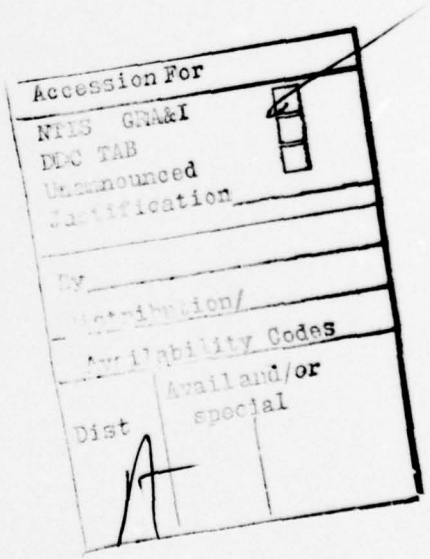

THEORY OF THE RESISTIVE HOSE INSTABILITY IN RELATIVISTIC ELECTRON BEAMS

I. Introduction

There is a large and growing literature on equilibrium[1] and stability[2-6] of intense relativistic electron beams propagating in initially neutral gas[7] or in preionized plasma.[8] The most serious magnetohydrodynamic instability of a beam in a resistive plasma channel appears to be the resistive hose (m = 1) instability.[7] This paper develops a Vlasov-Maxwell theory of the resistive hose instability in an infinitely long intense relativistic electron beam, propagating parallel to a uniform magnetic field $B_o \hat{e}_z$, with axial velocity $\beta_b c \hat{e}_z$ (Fig. 1). A dense background plasma is assumed to provide space charge neutralization, and the beam electron motion is taken to be paraxial ($p_z^2 \gg p_r^2 + p_\theta^2$), which requires that $\nu/\gamma_b \ll 1$, where ν is Budker's parameter and $\gamma_b mc^2$ is the characteristic energy of the beam electrons. Equilibrium and stability properties are calculated for rigid-rotor equilibria, which depend on energy H and canonical angular momentum P_θ exclusively through the linear combination $H - \omega_b P_\theta$, where ω_b is a constant, and for the related cold laminar flow equilibria, where ω_b can be a function of radial position r. Some of the results presented in this paper appear in the unpublished literature,[9] but are included as required for completeness.

Note: Manuscript submitted August 17, 1979.

Equilibrium properties are examined in Sec. II. In Sec. IIIA, an integro-differential eigenvalue equation is derived, assuming only that $k R_b \ll 1$, $\omega R_b \ll c$, and that there is complete space charge neutralization, where k, ω, and R_b are the axial wavenumber, frequency, and beam radius. The eigenvalue equation is reduced to an ordinary differential equation [Eq. (47)] in either the cold laminar flow limit, or in the case of a square radial density profile. By using a variational technique, an approximate dispersion relation [Eq. 64)],

$$\frac{i\omega}{c}\int_o^\infty dr\, r\, \sigma(r)\left(\frac{dA_o}{dr}\right)^2 = \int_o^\infty dr\, r\, \frac{dA_o}{dr}\,\frac{dJ_{bo}}{dr}\left(1+\frac{\omega_\beta^2(r)/(1-f_m)}{\Omega^2-\omega_c\Omega-\omega_\beta^2(r)}\right)$$

is obtained in Sec. IIID. [A slightly modified form holds when there is a conducting wall at R_c.] Here $\sigma(r)$ is the plasma electrical conductivity, $\omega_\beta(r)$ is the betatron frequency, ω_c is the cyclotron frequency associated with the field $B_o \hat{e}_z$, f is the fractional current neutralization of the equilibrium, and $A_o(r)\,\hat{e}_z$ and $J_{bo}(r)$ are the equilibrium vector potential and beam current density, respectively. The dispersion relation, Eq. (64), constitutes one of the main results of this paper, and can be used to investigate the resistive hose instability for a broad range of system parameters and arbitrary beam density profile. In the special case of a Bennett equilibrium profile, the dispersion relation can be further simplified to [Eq. (76)]

$$-i\omega\tau_d = \frac{f_m}{(1-f_m)^2} + \frac{6}{(1-f_m)^2}\,\frac{\bar{\Omega}^2}{\omega_{\beta m}^2}\left[\frac{1}{2} - \frac{\bar{\Omega}^2}{\omega_{\beta m}^2} + \frac{\bar{\Omega}^2(\omega_{\beta m}^2-\bar{\Omega}^2)}{\omega_{\beta m}^4}\ln\left(\frac{\omega_{\beta m}^2-\bar{\Omega}^2}{\bar{\Omega}^2}\right)\right],$$

where $\bar{\Omega}^2 \equiv \Omega^2-\omega_c\Omega$, τ_d is a characteristic diffusion time [Eq. (78)]

for the perturbed magnetic field, and $\omega_{\beta m} \equiv \omega_\beta(r = 0)$ is the maximum value of ω_β. This is a generalization (to include non-zero f_m and ω_c) of a result obtained by Lee[3] within the framework of a distributed-artificial-mass model. For a square beam profile, the dispersion relation reduces to

$$\bar{\Omega}^2 - \omega_\beta^2 = - \frac{\omega_\beta^2}{1-f_m} \frac{1-R_b^2/R_c^2}{1 - i\omega\tau_d(1-R_b^2/R_c^2)} ,$$

which also includes the effect of a conducting wall at R_c.

In Sec. IV, the stability properties are illustrated and discussed at length for a square beam profile, with particular emphasis on the influence of the applied field (ω_c), the conducting guide (through R_b/R_c), and the fractional current neutralization (f_m). It is found that the applied magnetic field and the finite channel radius strongly reduce the growth rate, whereas low frequency perturbations are considerably destabilized by even a small fractional current neutralization.

II. Equilibrium

We consider the equilibrium configuration illustrated in Fig. 1, consisting of an intense relativistic electron beam propagating parallel to a uniform applied magnetic field $B_{oz} \hat{\underset{\sim}{e}}_z$, through a background plasma whose conductivity varies with radial position. Cylindrical polar coordinates (r, θ, z) are used, with the z-axis along the axis of symmetry. Both the beam and plasma, in equilibrium, are assumed to be azimuthally symmetric $(\partial/\partial\theta = 0)$, infinitely long, and uniform axially $(\partial/\partial z = 0)$. The beam is characterized by density profile $n_{bo}(r)$, current density $J_{bo}(r)$, and number of electrons per unit length N_b and effective radius R_b, each defined by

$$N_b = 2\pi \int_o^\infty dr\, r\, n_{bo}(r) = \pi R_b^2\, n_{bo}(r = 0). \tag{1}$$

In this paper, we investigate the equilibrium and stability properties of steady state $(\partial/\partial t = 0)$ beam distributions of the form

$$f_{bo}(H, P_\theta, P_z) = F(H - \omega_b P_\theta)\, \delta(P_z - P_b), \tag{2}$$

where the total energy,

$$H = (m^2c^4 + p^2c^2)^{\frac{1}{2}} = \gamma mc^2, \tag{3}$$

the canonical angular momentum,

$$P_\theta = r(p_\theta - \tfrac{1}{2} eB_{oz} r/c), \tag{4}$$

and the axial canonical momentum,

$$P_z = p_z - \frac{e}{c} A_o(r) \tag{5}$$

are the three single particle constants of the motion. In the above, $\underset{\sim}{p} = (p_r, p_\theta, p_z)$ is the mechanical momentum, and -e and m are the electron charge and rest mass. $\underset{\sim}{A}_o(r) \equiv A_o(r)\,\hat{\underset{\sim}{e}}_z$ is the vector potential associated with the self-generated azimuthal magnetic field $B_\theta(r)$; from Ampere's law,

$$-\frac{1}{r}\frac{d}{dr}\,r\frac{d}{dr}A_o(r) \equiv \frac{1}{r}\frac{d}{dr}\,r\,B_{o\theta}(r)$$

$$= \frac{4\pi}{c}\left[J_{bo}(r) + J_{po}(r)\right] \qquad (6)$$

$$= \frac{4\pi}{c}(1 - f_m)\,J_{bo}(r),$$

where $J_{po}(r)$ is the axial plasma return current. For simplicity, we consider in this paper only the case where J_{po} is a uniform constant fraction f_m of $J_{bo}(r)$, as indicated in Eq. (6). We note that the distribution function (2) depends on H and P_θ exclusively through the linear combination $H - \omega_b P_\theta$, where ω_b is, in general, a constant. (In the cold fluid limit discussed below, each particle is localized to a particular value of r, and it is possible to allow ω_b to be a function of r, thus permitting sheared rotation.) The mean azimuthal motion of the beam electrons described by Eq. (1) corresponds to rigid rotation at angular velocity ω_b. It is assumed that the beam is completely space charge neutralized by the background plasma.

We assume in addition that the motion of the beam electrons is paraxial, i.e.

$$p_r^2 + p_\theta^2 \ll p_z^2. \qquad (7)$$

Inequality (7), which applies to the random component of electron motion as well as to ordered beam rotation, requires that

$$\frac{\nu}{\gamma_b} = \frac{N_b e^2 (1 - f_m)}{\gamma_b mc^2} \equiv \frac{I_{net}}{17{,}000\ \beta_b \gamma_b \text{ amps}} \ll 1, \tag{8}$$

where ν is known as Budker's parameter, $V_b \equiv \beta_b c$ and $\gamma_b mc^2$ are the characteristic beam electron axial velocity and energy, and I_{net} is the beam current less the plasma return current. It also follows from (7) that the axial self-generated magnetic field (due to beam rotation) can be neglected, since its dynamical influence is smaller than that of the azimuthal self-field by order p_θ^2/p_z^2. Thus the equilibrium magnetic field is taken to be

$$\underset{\sim}{B}_o(r) = B_{oz}\,\hat{\underset{\sim}{e}}_z + B_{o\theta}(r)\,\hat{\underset{\sim}{e}}_\theta, \tag{9}$$

where $B_{o\theta}(r)$ is determined by Eq. (6).

Using (7), it follows (after some straightforward algebra) that $H - \omega_b P_\theta$ can be approximated by

$$H - \omega_b P_\theta \approx \gamma_b mc^2 + \frac{p_\perp^2}{2\gamma_b m} + \psi_o(r), \tag{10}$$

where $\underset{\sim}{p}_\perp$ is the random component of transverse momentum,

$$p_\perp^2 \equiv p_r^2 + (p_\theta - \gamma_b mr\omega_b)^2, \tag{11}$$

the effective potential $\psi_o(r)$, associated with both magnetic and centrifugal forces, is

$$\psi_o(r) \equiv \tfrac{1}{2}\gamma_b mr^2\ [(\omega_b\omega_c - \omega_b^2) + \omega_\beta^2(r)], \tag{12}$$

$$\omega_\beta^2(r) \equiv 2e\beta_b A_o(r)/(\gamma_b m r^2) \tag{13}$$

is the squared betatron frequency (the electron oscillation frequency in the absence of beam rotation and of an axial B-field), $\omega_c \equiv eB_{oz}/m\gamma_b c$ is the beam electron cyclotron frequency, and the characteristic axial velocity of the beam is defined by

$$V_b \equiv \beta_b c \equiv P_b/\gamma_b m. \tag{14}$$

In (13) we have set $A(r = 0) = 0$, without loss of generality.

Making use of Eqs. (2) and (10), the beam density profile can be expressed as

$$n_{bo}(r) = 2\pi \gamma_b m \int_{\psi_o(r)}^{\infty} dU F(\gamma_b mc^2 + U), \tag{15}$$

where $U \equiv H - \omega_b P_\theta - \gamma_b mc^2$ is an effective transverse energy variable in the rotating frame of reference, and the lower limit of integration, $\psi_o(r)$, is the minimum possible value of U for an electron at r. To lowest order in $(p_r^2 + p_\theta^2)/p_z^2$, the mean axial velocity of the beam is approximated by V_b, defined in Eq. (14), and is independent of r. Similarly, we find that the mean azimuthal velocity is approximately

$$V_\theta(r) \equiv \int d^3r\, v_\theta f_{bo} \Big/ \int d^3p f_{bo} = \omega_b r, \tag{16}$$

corresponding to rigid rotation at constant angular velocity ω_b. From Eq. (6), and the constancy of V_b, we obtain the equilibrium azimuthal field

$$B_{o\theta}(r) = -4\pi e\beta_b(1 - f_m) r^{-1} \int_o^r dr'\, r'\, n_{bo}(r'). \tag{17}$$

From Eqs. (6), (13) and (17), $\omega_\beta^2(r)$ can also be written

$$\omega_\beta^2(r) = \frac{4\pi e^2 \beta_b^2}{\gamma_b m r^2} (1 - f_m) \int_o^r dr' r' n_{bo}(r'). \tag{18}$$

We also consider the case of cold laminar flow, characterized by

$$\frac{d\psi_o}{dr} = 0 \tag{19}$$

for all r. Substituting Eq. (12) into Eq. (19) and solving for ω_b, we find

$$\omega_b = \omega^{\pm}(r) = \tfrac{1}{2}\omega_c \pm [\tfrac{1}{4}\omega_c^2 + \omega_\beta^2(r)]^{\frac{1}{2}} . \tag{20}$$

The equilibrium described by Eqs. (2) and (20) is one in which each electron is localized near a particular value of r, performing a nearly circular helical orbit. Since r is a constant of the motion (to lowest order in $p_\perp^2/\gamma_b^2 m^2 r^2 \omega_b^2$), ω_b can be permitted to depend on r, giving sheared cold fluid rotation, rather than rigid rotation. The conditions $\omega_b = \omega^+(r)$ and $\omega_b = \omega^-(r)$ correspond respectively to fast and slow laminar rotation.

It will also be useful to rewrite Eq. (15) in the form

$$\frac{1}{r}\frac{dn_{bo}}{dr} = 2\pi\gamma_b m F[\gamma_b mc^2 + \psi_o(r)]\frac{1}{r}\frac{d\psi_o}{dr}$$

$$= 2\pi\gamma_b^2 m^2 F[\gamma_b mc^2 + \psi_o(r)][\omega^+(r) - \omega_b][\omega_b - \omega^-(r)]. \tag{21}$$

As a first example, we consider a loss cone distribution,

$$f_{bo}(H, P_\vartheta, P_z) = (n_b/2\pi\gamma_b m)\,\delta(H - \omega_b P_\vartheta - \gamma_o mc^2)\delta(P_z - P_b), \tag{22}$$

where γ_o is a constant satisfying $\gamma_o > \gamma_b$. Substituting Eq. (22) into Eq. (15), we find

$$n_{bo}(r) = \begin{cases} n_b, & 0 < r < R_b, \\ 0, & R_b < r < \infty, \end{cases} \tag{23a}$$

where R_b is defined by

$$R_b^2 = \frac{\gamma_b mc^2 r^2}{\psi(r)} \frac{\gamma_o - \gamma_b}{\gamma_b} \tag{23b}$$

and

$$\omega_\beta^2 = \frac{2\pi n e^2 \beta_b^2}{\gamma_b m} (1 - f_m), \tag{24}$$

so that ω_β and $\psi_o(r)/r^2$ are constants, independent of r.

The most familiar examples of beam equilibria with diffuse radial profiles occur when the beam electrons have a Gibbs distribution of "transverse energy", i.e.

$$f_{bo}(H, P_\theta, P_z) = \frac{n_b}{2\pi \gamma_b mT} \exp\left(\frac{H - \omega_b P_\theta - \gamma_o mc^2}{T}\right) \delta(P_z - P_b) . \tag{25}$$

For the case where the axial magnetic field is absent, $\omega_b = 0$, or where its effect is canceled by the centrifugal force of ordered beam rotation, $\omega_b = \omega_c$, the distribution function of Eq. (25) generates the familiar Bennett profile. Intense relativistic beam equilibria are discussed in many references.[1]

III. Linearized Vlasov-Maxwell Analysis

A. Derivation of the Integro-Differential Eigenvalue Equation

In this section, we use the linearized Vlasov-Maxwell equations to investigate the resistive hose (m = 1) instability of intense relativistic beam equilibria described by Eq. (2). We adopt a normal mode approach in which all perturbed quantities are assumed to vary with θ, z, and t as

$$\psi(\underset{\sim}{x}, t) = \hat{\psi}(r) \exp\left[i(\theta + kz - \omega t)\right] , \tag{26}$$

with $\mathrm{Im}\,\omega > 0$. In practice, it is often more convenient to use τ and z, rather than t and z, as independent variables, where

$$\tau \equiv t - z/V_b . \tag{27}$$

In this representation,

$$\psi(\underset{\sim}{x},t) = \hat{\psi}(r) \exp\left[i(\theta - \Omega z/V_b - \omega\tau)\right], \tag{26'}$$

where $\Omega \equiv \omega - kV_b$ is the frequency Doppler shifted to the beam frame. Either ω or Ω may be regarded as an externally determined quantity, depending on the situation envisioned. If, for example, a perturbation is initialized by a deflecting structure at z = 0, then ω is the real frequency of the deflector, and Ω, complex in general, represents the oscillation and growth (or damping) of the wave as a particular beam segment propagates downstream. If, on the other hand, each beam segment is taken to oscillate at a fixed real frequency Ω, then ω represents the growth of the wave as one moves backward from the head of the beam. Ω occurs through the dynamics of particular beam segments, and thus

scales with the natural oscillation frequencies of the beam electrons, ω_β and $\omega^\pm$, while ω occurs through the magnetic coupling of different beam segments, and thus scales with magnetic decay times.

We assume that the plasma is collisional to the extent that it is characterized by a real, scalar conductivity $\sigma(r)$. We further assume that the perturbed beam space charge field is completely neutralized by the plasma, which requires that

$$4\pi\sigma(r) \gg \omega, \tag{28}$$

for $r \lesssim R_b$, the beam radius. We consider only wavelengths long and frequencies low compared to quantities that characterize the beam radius, i.e.

$$|k R_b| \ll 1, \tag{29a}$$

$$|\omega R_b| \ll c, \tag{29b}$$

therefore

$$|\Omega R_b| \ll c. \tag{29c}$$

It follows that the transverse electric components of the perturbed fields, B_z, E_r, and E_θ, can be neglected, and the perturbation can be represented in terms of a perturbed axial component of vector potential $\hat{A}\,\hat{\underset{\sim}{e}}_z$:

$$\hat{B}_\theta(r) = -\frac{d\hat{A}(r)}{dr}, \tag{30a}$$

$$\hat{B}_r(r) = \frac{i}{r}\,\hat{A}(r), \tag{30b}$$

$$\hat{E}_z = -\frac{1}{c}\,\frac{\partial \hat{A}}{\partial t}. \tag{30c}$$

After some algebraic manipulation, Ampere's law for $\hat{A}(r)$ can be expressed as

$$\frac{d}{dr}\,\frac{1}{r}\,\frac{d}{dr}\,r\hat{A} + \frac{4\pi\, i\omega\, \sigma(r)}{c^2}\,\hat{A} = -\,\frac{4\pi}{c}\,\hat{J}_b(r)\,, \tag{31}$$

where $\hat{J}_b(r)$ is the perturbed axial beam current density,

$$\hat{J}_b(r) = -\,e\int d^3p\, v_z \hat{f}_b(r,p), \tag{32}$$

and the perturbed beam electron distribution is given by

$$\hat{f}_b(\underset{\sim}{x},\underset{\sim}{p}) = e\int_{-\infty}^{0} d\tilde{\tau}\, \exp\,(-\,i\omega\,\tilde{\tau}\,)\,\frac{\underset{\sim}{v}' \times \hat{\underset{\sim}{B}}\,(\underset{\sim}{x}')}{c}\cdot\frac{\partial f_{bo}(x',p')}{\partial p'}\,. \tag{33}$$

In Eq. (33), $\tilde{\tau} \equiv \tau - \tau$, and $\underset{\sim}{x}'(\tau')$, $\underset{\sim}{v}'(\tau')$ traces the unperturbed electron trajectories backward in time, given the initial conditions $\underset{\sim}{x}'(\tau' = \tau) = \underset{\sim}{x}$, $\underset{\sim}{v}'(\tau' = \tau) = \underset{\sim}{v}$. Using (30) to substitute $\hat{A}$ for $\hat{B}$, and performing some straightforward algebra, we find

$$\hat{f}_b(r,\underset{\sim}{p}) = \frac{ep_z}{p_\perp c}\,\frac{\partial f_{bo}}{\partial p_\perp}\left\{\hat{A}(r) + (\Omega-\omega_b)\int_{-\infty}^{0} d\tilde{\tau}\; i\,\hat{A}(r')\exp[\,i(\theta'-\theta-\tilde{\tau})]\right\}. \tag{34}$$

We next introduce the polar momentum variables $(p_\perp, \phi)$ in the rotating frame, defined by

$$\begin{aligned} p_x + \gamma_b m\omega_b y &= p_\perp \cos\phi\,, \\ p_y - \gamma_b m\omega_b x &= p_\perp \sin\phi\,, \end{aligned} \tag{35}$$

where $p_\perp$ is defined in Eq. (11), and the Cartesian coordinates (x, y) are related to the polar coordinates (r, θ) by $x = r\cos\theta$ and $y = r\sin\theta$. Substituting Eq. (34) into Eq. (32), and making use of

Eqs. (7) and (35), the eigenvalue equation (31) for resistive hose instability can be expressed as

$$\frac{d}{dr}\ \frac{1}{r}\frac{d}{dr}\,r\hat{A} + \frac{4\pi\sigma}{c}\left(\frac{i\omega}{c}\right)\ \hat{A}$$

$$= 8\pi^2\,\gamma_b m e^2 \beta_b{}^2 \int_0^\infty dp_\perp \frac{\partial}{\partial p_\perp} F(H - \omega_b p_\theta)\,[\hat{A}(r) + (\Omega - \omega_b)I]\ , \qquad (36a)$$

where the orbit integral I is defined by

$$I = i\int_0^{2\pi}\frac{d\phi}{2\pi}\int_{-\infty}^{0} d\tilde{\tau}\hat{A}(r')\ \exp\{\,i[(\theta' - \theta\ ) - \Omega\,\tilde{\tau}\ ]\}\ . \qquad (36b)$$

The integro-differential eigenvalue equation (36) constitutes one of the main results of this paper and can be used to investigate stability properties for a broad range of system parameters. We emphasize that Eq. (36) has been derived with no <u>a priori</u> assumption that the beam is cold, or uniform, or that the perturbation is a rigid displacement.[2,3] However, on each of these limiting cases, Eq. (36) can be simplified considerably, as discussed in the remainder of this section.

B. Cold Fluid Description

The orbit integral I and corresponding eigenvalue equations are obtained in this section for the cold fluid equilibrium. Substituting the identity

$$\hat{A}(r') = \int_0^\infty dr'' \; r'' \; \hat{A}(r'') \int_0^\infty d\lambda \; \lambda \; J_1(\lambda r') \; J_1(\lambda r'')$$

into Eq. (36b), we have

$$I = \frac{1}{2\pi} \int_0^\infty dr'' \; r'' \; \hat{A}(r'') \int_0^\infty d\lambda \; \lambda \; J_1(\lambda r'') \int_0^\infty id\tilde{\tau} \; \exp(-i\Omega\tilde{\tau}) \cdot \int_0^{2\pi} d\phi \; J_1(\lambda r') \exp[i(\theta' - \theta)] \tag{37}$$

where J_ℓ is the Bessel function of the first kine of order ℓ. Defining

$$\lambda_x = \lambda \cos\alpha, \qquad \lambda_y = \lambda \sin\alpha,$$

$J_1(\lambda r') \exp[i(\theta' - \theta)]$ in Eq. (37) can be expressed in terms of the Cartesian orbits $x'(\tau) = r'(\tau)\cos\theta'(\tau)$ and $y'(\tau) = r'(\tau)\sin\theta'(\tau)$ as

$$J_1(\lambda r') \exp\{i(\theta' - \theta)\} = \int_0^{2\pi} \frac{d\alpha}{2\pi} \exp[i(\alpha - \theta - \frac{\pi}{2})] \exp(i\lambda_x x' + i\lambda_y y') \tag{38}$$

In the cold fluid limiting case, the unperturbed transverse orbits $[r'(\tilde{\tau}), \theta'(\tilde{\tau})]$ of the beam electrons are near circular, i.e. $r' \approx r$. It follows that the deviations from circularity, of order

$$p_\perp^2/\gamma_b^2 m^2 R_b^2 (\omega^+ - \omega^-)^2 << 1, \tag{39}$$

are simple harmonic, and the unperturbed orbits are given by[10]

$$x'(\tilde{\tau}) = \frac{1}{\omega^+ - \omega^-} \frac{p_\perp}{\gamma_b m} \left[\sin(\phi + \omega^+ \tilde{\tau}) - \sin(\phi + \omega^- \tilde{\tau})\right]$$

$$+ r(\omega_b - \omega^-) \cos(\theta + \omega^+ \tilde{\tau}) - r(\omega_b - \omega^+) \cos(\theta + \omega^- \tilde{\tau}) \tag{40a}$$

$$y'(\tilde{\tau}) = \frac{1}{\omega^+ - \omega^-} \left\{ \frac{p_\perp}{\gamma_b m} \left[\cos(\phi + \omega^- \tilde{\tau}) - \cos(\phi + \omega^+ \tilde{\tau})\right] \right.$$

$$\left. + r(\omega_b - \omega^-) \sin(\theta + \omega^+ \tilde{\tau}) - r(\omega_b - \omega^+) \sin(\theta + \omega^- \tilde{\tau}) \right\}, \tag{40b}$$

where the biharmonic frequencies ω^+ and ω^-, evaluated at r, are the fast and slow laminar rotation frequencies defined in Eq. (20). Substituting Eqs. (40) into Eq. (38) and carrying out the integration over ϕ, we have

$$\int_0^{2\pi} \frac{d\phi}{2\pi} J_1(\lambda r') \exp\left\{i(\theta' - \theta)\right\} = \int_0^{2\pi} \frac{d\alpha}{2\pi} \exp\left[i(\alpha - \theta - \frac{\pi}{2})\right]$$

$$\cdot \exp\left\{ \frac{r(\omega_b - \omega^-)}{\omega^+ - \omega^-} \left[\lambda_x \cos(\theta + \omega^+ \tilde{\tau}) + \lambda_y \sin(\theta + \omega^+ \tilde{\tau})\right] \right. \tag{41}$$

$$\left. + \frac{r(\omega^+ - \omega_b)}{\omega^+ - \omega^-} \left[\lambda_x \cos(\theta + \omega^- \tilde{\tau}) + \lambda_y \sin(\theta + \omega^- \tilde{\tau})\right] \right\},$$

where the cold fluid approximation (39) has been invoked. Similarly, the integration over α in Eq. (41) gives

$$\int_0^{2\pi} \frac{d\phi}{2\pi} J_1(\lambda r') \exp\left\{i(\theta' - \theta)\right\}$$

$$= J_1\left[\frac{\lambda r}{\omega^+ - \omega^-} \chi(\tilde{\tau})\right] \left\{ \frac{\omega_b - \omega^-}{\chi(\tilde{\tau})} \exp(i\omega^+ \tilde{\tau}) + \frac{\omega^+ - \omega_b}{\chi(\tilde{\tau})} \exp(i\omega^- \tilde{\tau}) \right\} \tag{42}$$

where the effective frequency difference $\chi(\tilde{\tau})$ is defined by

$$\chi(\tilde{\tau}) = [(\omega_b - \omega^-)^2 + (\omega^+ - \omega_b)^2 + (\omega_b - \omega^-)(\omega^+ - \omega_b) \sin(\omega^+ - \omega^-)\tilde{\tau}\,]^{\frac{1}{2}} . \quad (43)$$

However, the cold fluid limiting case is characterized by laminar rotation[10] at either ω^- or ω^+, i.e.

$$\omega_b \approx \omega^-, \text{ or } \omega_b \approx \omega^+ ; \quad (44)$$

thus

$$\chi(\tilde{\tau}) \approx \omega^+ - \omega^- . \quad (45)$$

Substituting Eqs. (42) and (45) into Eq. (37), and carrying out the integration over time and r'', we obtain

$$I = -\hat{A}(r)\left[\frac{\omega_b - \omega^-}{\omega^+ - \omega^-}\,\frac{1}{\Omega - \omega^+} + \frac{\omega^+ - \omega_b}{\omega^+ - \omega^-}\,\frac{1}{\Omega - \omega^-}\right] , \quad (46)$$

which is independent of $p_\perp$. We note that both terms in (46) are essential, even though (44) indicates that one of the terms is much larger than the other; the larger term almost cancels out when inserted in (36a).

The integration over $p_\perp$ in Eq. (36a) is now trivial, since the term in brackets is independent of $p_\perp$. Using Eq. (21) to eliminate F in terms of $J_{bo}(r)$, we find (after some algebra) the eigenvalue equation for the cold fluid limit,

$$\frac{d}{dr}\,\frac{1}{r}\,\frac{d}{dr}\,r\hat{A}(r) + \frac{4\pi i\omega\sigma(r)}{c^2}\,\hat{A}(r) = \frac{4\pi\, e\beta_b}{\gamma_b mc}\,\frac{\hat{A}(r)}{[\Omega - \omega^-(r)][\Omega - \omega^+(r)]}\,\frac{1}{r}\,\frac{dJ_{bo}}{dr} , \quad (47)$$

where $\omega^\pm(r)$ are given by Eqs. (20) and (18), in terms of the radial profile of beam density $n_{bo}(r)$ or current density $J_{bo}(r)$. The treatment of

the singularities in Eq. (47) is determined by the requirement that Ω be in the upper half plane. The boundary conditions on Eq. (47) are

$$\hat{A}(0) = \hat{A}(R_c) = 0, \tag{48}$$

where R_c may be ∞ if the beam propagates in a conducting plasma of infinite extent, or is finite if there is a perfectly conducting guide at $r = R_c$. Of course, the case of finite R_c makes sense only if $J_{bo}(R_c)=0$. Equations (47) and (48) determine the hose stability properties of any beam current density profile $J_{bo}(r)$, provided that the beam electrons are in a cold laminar flow equilibrium.

C. Uniform Beam with Sharp Boundaries

In Eq. (36), we have obtained an eigenvalue equation that is very generally valid. However the source term in Eq. (36) contains an integral of the unknown eigenfunction $\hat{A}(r)$ over unperturbed orbits, which makes the equation rather intractable in general. This difficulty is fundamental, reflecting the fact that individual electron orbits span the beam cross-section, communicating information about the perturbation from one value of r to another. In Sec. IIIB, we avoided the problem by considering a cold, differentially rotating beam equilibrium, in which each individual electron is confined to a narrow range of r; Eq. (36) then reduced to the ordinary differential equation (47). In this section, we begin to explore a different approach in which the orbit integral is evaluated approximately by taking advantage of simplifications [periodic orbits, smoothly varying $\hat{A}(r)$] that arise naturally. In this section, we consider only the case of a beam with uniform density out to a sharp boundary at $r = R_b$, for which this approach is most straightforward. (More general density profiles will be considered in subsequent papers.) We do not assume here that the beam is cold; nevertheless, for the uniform density beam, we arrive at the same eigenvalue equation (47). For generality, we continue to permit the presence of a guide field B_{oz}, a conducting guide at $r = R_c$ (where R_c may be allowed to go to ∞), and an equilibrium return current density $f_m J_{bo}$.

For any given value of Ω (which plays the role of k_z in the usual three-dimensional eigenvalue problem), there is in general an infinite sequence of eigenvalues ω, corresponding to different values

of the radial quantum number [the number of oscillations in $\hat{A}(r)$]. Our interest lies in the lowest eigenfunction, which corresponds to a sideways displacement of the whole beam, and is expected to be the most unstable mode. In the low frequency limit,

$$4\pi\sigma R_b^2 \left| \omega \right| /c^2 \ll 1, \tag{49}$$

this eigenfunction becomes

$$\hat{A}(r) \propto r, \tag{50}$$

representing a rigid displacement of the uniform beam as well as the self-generated B_θ field. For ω large enough that

$$4\pi\sigma R_b^2 \omega/c^2 \gtrsim 1,$$

magnetic diffusion begins to distort the eigenfunction $\hat{A}(r)$, even if the beam itself were to displace rigidly. Nevertheless, $\hat{A}(r)$ follows (50) closely at the origin and over much of the beam, bending over somewhat for larger r, as illustrated in some examples at the end of this section. As we shall see, the inequality (49) holds, but not as a strong inequality, over the whole range of strongest instability.

In view of this discussion, and particularly since the integral in Eq. (36b) is merely an average over $\hat{A}(r)$, and is not expected to depend strongly on the detailed structure of $\hat{A}(r)$, we use the assumed form

$$\hat{A}(r') = \hat{A}(r)r'/r \tag{51}$$

in the integrand of (36b). Equation (51) is correct at $r' = r$, as well

as having the right form at the origin, and becoming exact for either small r or small ω.

For a uniform beam, ω_β and $\omega^\pm$ are independent of r, and it is easy to show that the unperturbed orbits are given exactly by the simple harmonic forms of Eq. (40). Using Eq. (51), Eq. (36b) reduces to

$$\begin{aligned} I &= i\hat{A}(r)r^{-1}\int_{-\infty}^{0} d\tilde{\tau}\, \exp(-i\theta - i\Omega\tilde{\tau}) \int_0^{2\pi} (d\phi/2\pi) r' e^{i\theta'} \\ &= i\hat{A}(r)r^{-1}\int_{-\infty}^{0} d\tilde{\tau}\, \exp(-i\theta + i\Omega\tilde{\tau}) \int_0^{2\pi} (d\phi/2\pi)(x' + iy'), \end{aligned} \tag{52}$$

and using Eqs. (40) for the orbits (x', y'), the integrals in Eq. (52) are easily performed. The result is identical with Eq. (46). Thus Eq. (47) also holds, and explicitly inserting the uniform beam current density, we arrive at the eigenvalue equation

$$\frac{d}{dr}\frac{1}{r}\frac{d}{dr} r\hat{A}(r) + \frac{4\pi i\sigma(r)\omega}{c^2}\hat{A}(r) = \frac{\omega_{pb}^2\beta_b^2}{(\Omega-\omega^-)(\Omega-\omega^+)}\frac{\delta(r-R_b)}{r}\hat{A}(r), \tag{53}$$

where

$$\omega_{pb} \equiv (4\pi ne^2/m\gamma_b)^{\frac{1}{2}}$$

is the beam plasma frequency; we note that, for a uniform beam,

$$\omega_\beta^2 = \tfrac{1}{2}\omega_{pb}^2\beta_b^2(1 - f_m).$$

The appropriate boundary conditions are again those of Eq. (48). We note that if Eq. (49) holds, the eigenfunction $\hat{A}(r)$ within the beam is indeed given by Eq. (50), as discussed previously.

If $\sigma(r)$ is a constant σ within the beam, and a (possibly different) constant σ_1 outside the beam, the eigenfunctions of (53)

are Bessel functions of order one, and a dispersion relation connecting ω and Ω is easily derived in closed form, from the boundary conditions (48) as well as the matching conditions at $r = R_b$. We consider the particular case

$$\sigma(r) = \begin{cases} \sigma(\text{const}), & 0 < r < R_b, \\ \sigma_1 << c^2/4\pi R_b^2 \omega, & R_b < r < R_c. \end{cases} \tag{54}$$

The condition on σ_1 in Eq. (54) insures that magnetic diffusion through the weakly conducting region $R_b < r < R_c$ is slow compared to the time scale ω^{-1}, and thus that terms in the dispersion relation proportional to σ_1 are negligibly small. Strictly speaking, σ_1 cannot be zero, since our assumption of electrostatic neutrality requires that $4\pi \sigma_1 > \omega$ is easily compatible with (54), according to Eq. (28). Cases in which $4\pi\sigma$ falls below ω for r greater than some radius R_o can easily be treated by applying appropriate boundary conditions at R_o, as discussed by Lee.[3]

For a beam of radius R_b, with $\sigma(r)$ given by Eq. (54),

$$\hat{A}(r) = J_1(\kappa r) \qquad , 0 \le r \le R_b, \tag{55a}$$

$$\hat{A}(r) = \frac{R_b}{r} \frac{R_c^2 - r^2}{R_c^2 - R_b^2} J_1(\kappa R_b), \quad R_b \le r \le R_c, \tag{55b}$$

where

$$\kappa^2 \equiv 4\pi i \sigma \omega / c^2 \tag{56}$$

and the dispersion relation is

$$(\Omega - \omega^-)(\Omega - \omega^+) = \omega_{pb}^2 \beta_b^2 F_1(\omega), \tag{57a}$$

or equivalently,

$$\Omega^2 - \omega_c\Omega - \omega_\beta^{\,2} = \omega_{pb}^{\,2}\beta_b^{\,2}F_1(\omega), \tag{57b}$$

with

$$F_1(\omega) = -\left(\kappa R_b \frac{J_1'(\kappa R_b)}{J_1(\kappa R_b)} + \frac{R_c^{\,2} + R_b^{\,2}}{R_c^{\,2} - R_b^{\,2}}\right)^{-1} . \tag{57c}$$

The properties of the dispersion relation (57) are illustrated and discussed in Sec. IV, with particular emphasis on the effects of the B_{zo} guide field, the conducting guide at R_c, and the plasma return current $J_{po}(r) = - f_m J_{bo}(r)$.

D. Variational Approximation to the Dispersion Relation

Except in special cases such as the uniform density beam with a sharp boundary, considered in Sec. III C, the eigenvalues and eigenfunctions of Eq. (47) can only be calculated numerically. Such solutions will be presented in future publications. In this section, we develop a variational technique of approximating the eigenvalues that is widely applicable.

Beginning with Eq. (47), we multiply through by $rA(r)$ and integrate over r, to obtain

$$\frac{4\pi i\,\omega}{c^2}\int_0^{R_c} dr r\sigma(r)\hat{A}^2(r)$$
$$= \int_0^{R_c} dr r\left[\frac{4\pi e\beta_b}{mc\gamma_b}\;\frac{\hat{A}^2(r)}{(\Omega-\omega^-)(\Omega-\omega^+)}\;\frac{1}{r}\;\frac{dJ_{bo}}{dr} - \hat{A}(r)\,\frac{d}{dr}\frac{1}{r}\frac{d}{dr}\,r\,\hat{A}(r)\right]. \quad (58)$$

If we guess a trial form $\hat{A}^t(r)$ for the eigenfunction, and

$$\hat{A}^t(r) \equiv \hat{A}(r) + \delta\hat{A}(r), \quad (59)$$

where $\hat{A}(r)$ is the (unknown) exact solution, let ω^t be the eigenvalue calculated (for given Ω) by using $\hat{A}^t(r)$ in Eq. (58). We also let

$$\omega^t \equiv \omega + \delta\omega \quad (60)$$

where ω is the (unknown) exact eigenvalue. We find then, after two integrations by parts, that

$$\frac{4\pi i\delta\omega}{c^2}\int_0^{R_c} dr\, r\sigma(r)\,\hat{A}^2(r)$$
$$= -\int_0^{R_c} dr r\delta\hat{A}(r)\left[\frac{4\pi i\omega\sigma(r)}{c^2} - \frac{4\pi}{c}\frac{e\beta_b}{m\gamma_b}\frac{1}{(\Omega-\omega^-)(\Omega-\omega^+)}\frac{1}{r}\frac{dJ_{bo}}{dr} + \frac{d}{dr}\frac{1}{r}\frac{d}{dr}\,r\right]\delta\hat{A}(r), \quad (61)$$

provided that the trial eigenfunction $\hat{A}^t(r)$ satisfies the required boundary conditions (48). Thus the first variation

$$\frac{\delta\omega}{\delta\hat{A}(r)} = 0, \tag{62}$$

and the calculated eigenvalue ω^t is accurate to second order in the error $\delta\hat{A}$.

However, the differential operator in Eq. (47) is non-Hermitian, because Im $\Omega > 0$; consequently both ω and $\hat{A}(r)$ are complex, and the condition (62) determines a saddle point in the complex plane, rather than an extremum, as in the usual case of a Hermitian operator, where the eigenvalue and eigenfunction are real. As a result, the error $\delta\omega$, although small, is not positive definite, as would be true for a Hermitian operator, i.e. one cannot simply seek a trial function $\hat{A}^t$ that minimizes ω^t. Nevertheless, Eq. (61) is valuable if one can find a trial eigenfunction that is even qualitatively correct, since the error in ω^t is second order. An obvious choice for this purpose is to use the form of $\hat{A}^t(r)$ corresponding to a rigid displacement of the magnetic field,

$$\hat{A}^t(r) \propto dA_o/dr, \tag{63}$$

provided that the outer boundary condition is at $R_c = \infty$. [If R_c is finite, a slightly modified choice of $\hat{A}^t$ is required to satisfy the boundary condition $\hat{A}(R_c) = 0$, Eq. (48), as will be discussed.] We then find that Eq. (58) reduces to the dispersion relation

$$\frac{i\omega}{c}\int_o^\infty dr r\sigma(r)\left(\frac{dA_o}{dr}\right)^2 = \int_o^\infty dr r \frac{dA_o}{dr}\frac{dJ_{bo}}{dr}\left(1 + \frac{\omega_\beta^2(r)(1-f_m)^{-1}}{[\Omega-\omega^-(r)][\Omega-\omega^+(r)]}\right), \tag{64}$$

where the identity

$$(\Omega-\omega^-)(\Omega-\omega^+) \equiv \Omega^2-\omega_c\Omega-\omega_\beta{}^2 \tag{65}$$

has been used.

We consider two special cases; the first is the beam with a square radial density profile, also discussed in Sec. III C. For this case we consider also the presence of a conducting guide at R_c. The natural choice for a trial eigenfunction is then

$$\hat{A}^t(r) = \begin{cases} r & , \quad 0 \le r \le R_b. \\ \dfrac{R_b{}^2}{R_c{}^2-R_b{}^2}\left(\dfrac{R_c{}^2}{r} - r\right) & , \quad R_b \le r \le R_c, \end{cases} \tag{66}$$

which satisfies (63) for $r < R_b$, but not for $r > R_b$, and also satisfies (48). Equation (58) then reduces to a dispersion relation that is slightly different from (64),

$$\frac{1}{1-R_b{}^2/R_c{}^2} + \frac{\omega_{pb}{}^2\beta_b{}^2}{(\Omega-\omega^-)(\Omega-\omega^+)} = \frac{2\pi i\omega}{R_b{}^2c^2}\left[\int_0^{R_b} drr^3\sigma(r)\right. \tag{67}$$

$$\left. + \frac{R_b{}^4}{(R_c{}^2-R_b{}^2)^2}\int_{R_b}^{R_c}\frac{dr}{r}\,(R_c{}^2-r^2)^2\,\sigma(r)\right] .$$

Specializing still further to the piece-wise flat conductivity profile of Eq. (54), the dispersion relation (67) can be put in the form

$$(\Omega-\omega^-)(\Omega-\omega^+) = \omega_{pb}{}^2\beta_b{}^2\,F_2(\omega), \tag{68a}$$

with

$$F_2(\omega) \equiv - \frac{1-R_b^2/R_c^2}{1-i\omega\tau_d(1-R_b^2/R_c^2)}, \tag{68b}$$

where τ_d, essentially a decay time for the perturbed current, is defined for this case by

$$\tau_d = \tfrac{1}{2}\pi\sigma R_b^2/c^2 = -\tfrac{1}{8}i\kappa^2 R_b^2/\omega \ , \tag{69}$$

and κ is the quantity defined in Eq. (56). Equation (68a) is in exactly the same form as the exact solution of (47) for this particular beam and conductivity profile, Eq. (57), except that an approximate function $F_2(\omega)$ from (68b) replaces the exact result $F_1(\omega)$ from (57c). To check on the accuracy of the approximation $F_2(\omega)$, we note that $F_1(\omega)$, expanded in powers of $\omega\tau_d$ up to second order, is

$$F_1(\omega) \approx - \frac{1 - R_b^2/R_c^2}{1 + (- i\omega\tau_d + \frac{1}{6}\omega^2\tau_d^2)(1 - R_b^2/R_c^2)} \ . \tag{70}$$

We see that F_1 and F_2 are identical up to a numerically small correction of order $\omega^2\tau_d^2$; thus the dispersion relation of Eq. (68) is an excellent approximation for $\omega\tau_d \lesssim 1$. This is as might be expected, since the model of rigid displacement is qualitatively accurate in this regime, which is expected to include the fastest growing modes.

Alternatively, Eqs. (68a, b) can be written in the forms

$$\omega\tau_d = -i \left(1 - \frac{R_b^2}{R_c^2}\right)^{-1} - \frac{i\,\omega_{pb}\beta_b^2}{(\Omega-\omega^-)(\Omega-\omega^+)} \tag{68c}$$

$$\equiv -i\left(1-\frac{R_b^2}{R_c^2}\right)^{-1} - \frac{i\omega_{pb}^2\beta_b^2}{\bar{\Omega}^2-\omega_\beta^2} , \qquad (68d)$$

where

$$\bar{\Omega}^2 \equiv \Omega(\Omega-\omega_c) . \qquad (71)$$

The dependence of ω on Ω is given explicitly by Eqs. (68c, d). We note the following features: (i) For Ω real, ω is pure imaginary. Instability ($\mathrm{Im}\,\omega > 0$) occurs only over a bounded range of Ω, which is a subset of the range $\omega^- < \Omega < \omega^+$. (ii) The growth rate $\mathrm{Im}\,\omega$ goes to infinity as $\Omega \to \omega^-$ from above or $\Omega \to \omega^+$ from below. This occurs for a flat beam profile, because all beam electrons are in resonance with the wave at these frequencies. For rounded beam profiles[3], the growth rate is finite for any value of Ω, as will be illustrated. (iii) Increasing the return current is destabilizing, since $\omega_{pb}^2\beta_b^2/\omega_\beta^2 = 2/(1-f_m)$. Proximity to the wall, i.e. increasing R_b/R_c, is stabilizing. The effect of a B_z guide field is merely to substitute $\bar{\Omega}^2$ for Ω^2, as is evident from Eqs. (47) and (65) for any beam profile. Thus the growth spectrum $\mathrm{Im}\,\omega$, for Ω on the real line, is shifted to different values of Ω by the presence of a guide field. However, we shall see that B_z is stabilizing when Ω is calculated as a function of real ω. The stability properties are discussed further in Sec. IV, particularly for real ω, and with emphasis on the effects of the conducting guide, the plasma return current, and the B_z field.

As a second example, we consider the Bennett profile,

$$n_{bo}(r) = n_{bo}(0)(1 + r^2/R_b^2)^{-2} \qquad (72)$$

which is the equilibrium profile for a paraxial, monoenergetic, non-rotating beam subject to isotropic small angle scattering by a uniform plasma medium. In this case, the dispersion relation (64) reduces to

$$\int_0^1 d\eta\eta(1-\eta)\ \frac{\Omega^2-\omega_c\Omega+\eta\,\omega_{\beta m}{}^2 f_m/(1-f_m)}{\Omega^2-\omega_c\,\Omega-\eta\,\omega_{\beta m}{}^2} = \frac{i\pi R_b{}^2\omega}{2c^2}(1-f_m)\int_0^1 d\eta\ \frac{1-\eta}{\eta}\,\sigma\,(\eta), \quad (73)$$

where the variable of integration is

$$\eta = (1 + r^2/R_b{}^2)^{-1} \quad , \quad (74)$$

and $\omega_{\beta m}$ is the maximum value of ω_β,

$$\omega_{\beta m} = \omega_\beta(r = 0) \ . \quad (75)$$

Performing the integration in Eq. (73), we obtain

$$\omega\tau_d = i\ (1-f_m)^{-2}\ [f_m + G(\bar{\Omega}^2/\omega_{\beta m}{}^2)] \quad , \quad (76a)$$

where

$$G(x) \equiv 6x\ [\tfrac{1}{2} - x + x(1-x)\ \ell n\ (\tfrac{1-x}{x})] \ , \quad (76b)$$

and a magnetic diffusion time is defined by

$$\tau_d = (3\pi R_b{}^2/c^2)\int_0^1 d\eta(\eta^{-1} - 1)\ \sigma\ (\eta) \quad . \quad (77)$$

Equation (76) has branch points at $\bar{\Omega}^2 = 0$ and $\bar{\Omega}^2 = \omega_{\beta m}{}^2$. To satisfy causality (Im $\Omega > 0$), on the real $\bar{\Omega}^2$ axis we define

$$\ell n\left(\frac{\omega_{\beta m}{}^2-\bar{\Omega}^2}{\bar{\Omega}^2}\right) = \ell n\ \left|\ \frac{\omega_{\beta m}{}^2-\bar{\Omega}^2}{\bar{\Omega}^2}\ \right| + ig\,\pi \ , \quad (78)$$

where

$$g = 0, \text{ if } \quad \omega_{\beta m}^2 < \bar{\Omega}^2 \tag{79a}$$

$$g = 0, \text{ if } \quad \bar{\Omega}^2 < 0 \text{ (equivalent to } 0 < \Omega < \omega_c), \tag{79b}$$

$$g = -1, \text{ if } \quad 0 < \bar{\Omega}^2 < \omega_{\beta m}^2, \text{ and } \Omega < 0, \tag{79c}$$

$$g = +1, \text{ if } \quad 0 < \bar{\Omega}^2 < \omega_{\beta m}^2, \text{ and } 0 < \Omega \text{ (requires } \omega_c < \Omega). \tag{79d}$$

For the special case with

$$f_m = 0, \tag{80a}$$

$$\omega_c = 0, \tag{80b}$$

and

$$\sigma(r) = \sigma_c \, (1 + r^2/R_b^2)^{-2}, \tag{81}$$

Eqs. (76) and (77) reduce to the dispersion relation previously discussed in detail by Lee,[3] who arrived at this result by using an entirely different set of plausibility arguments--principally a model in which the beam is sliced into overlapping rigid disks with an artificial distribution of particle mass.

The function $G(\bar{\Omega}^2/\omega_{\beta m}^2)$ is displayed in Fig. 2, for $\bar{\Omega}^2$ real. In contrast to the beam with square radial profile, discussed previously, the growth rate Im ω is bounded (because the natural oscillation frequencies $\omega^{\pm}$ vary for different electrons, and there is no single frequency Ω for which the entire beam is resonant with the wave). Another difference is that, from Eq. (79), ω is complex in the range $0 < \bar{\Omega}^2 < \omega_{\beta m}^2$. Equation (76a) also exhibits explicitly the dependence

on the current neutralization factor f_m. For $f_m = 0$, only the range $0 < \bar{\Omega}^2 < \frac{1}{2}\omega_{\beta m}{}^2$ is unstable, but as $f_m \to 1$, the entire range $-\infty < \bar{\Omega}^2 \leq 0.65\,\omega_{\beta m}{}^2$ becomes unstable. [According to Eq. (70), negative values of $\bar{\Omega}^2$ up to $-\frac{1}{4}\omega_c{}^2$ occur for Ω in the range $0 < \Omega < \omega_c$.] Growth rates $\mathrm{Im}\,\omega$ also go to infinity as $f_m \to 1$. The destabilizing effect of f_m is due to the repulsive interaction between the beam current and the return current; it is particularly striking and significant that instability can occur even for $\Omega = 0$, when $f_m > 0$.

IV. Effects of Guide Field, Conducting Walls, and Current Neutralization

In this section, we present an analysis of the hose stability properties of the beam with uniform density to radius R_b, in the narrow conducting channel of Eq. (54). The dispersion relation is plotted in a variety of ways, to illustrate the effects of the applied B_z field, the fractional neutralization of the equilibrium beam current (f_m), and the conducting guide at R_c. Some of the results in this section are similar to previous work reported in the unpublished literature,[9] but are presented here for completeness. We concentrate on the region $\omega T_d \leq 1$ of parameter space, where the approximate dispersion relation of Eq. (68), is essentially indistinguishable from the exact result, Eq. (57), from which results are plotted, and where the beam displaces essentially rigidly.

Depending upon the way in which a stability problem is phrased (initial value problem in beam or laboratory frame, driven oscillation) either Ω or ω may be regarded as the independent variable, and taken to be real; for general understanding of convective properties of the wave, it is necessary to treat both variables in the complex plane. However most experiments are performed by "tickling" the beam, at real frequency ω, at a particular location z. Im Ω then determines the growth of the wave, on a particular beam segment, as the beam propagates downstream. Our discussion here will thus be in the form $\Omega(\omega)$, where ω is real.

We note again, from Eqs. (57b), (64) and (65), that the effect of the guide field is to replace Ω^2 with $\bar{\Omega}^2 \equiv \Omega\,(\Omega - \omega_c)$ in the dispersion

relation. Thus, if ω is regarded as a function of real Ω, the guide field does not reduce the maximum growth rate Im ω, but merely shifts it to a different value of Ω. On the other hand, for a given real value of ω, the replacement reduces the growth rate Im Ω, as will be amply illustrated, and thus can be regarded as stabilizing in this sense.

We consider first the case $\omega\tau_d \to 0$, i.e. low frequency or very high resistivity. The dispersion relation then reduces to

$$2\frac{\Omega^2 - \omega_c\Omega}{\omega_{pb}^2\beta_b^2} + f_m - \frac{R_b^2}{R_c^2} = 0, \tag{82}$$

whence a necessary and sufficient condition for instability is

$$f_m > \frac{R_b^2}{R_c^2} + \tfrac{1}{2}\frac{\omega_c^2}{\omega_{pb}^2\beta_b^2}, \tag{83}$$

a result that is illustrated in Fig. 3. It is indeed remarkable that instability occurs even in this limit. The reason, of course, is that the beam tends to be expelled from the highly conducting central region of the channel by the return current. This effect is particularly strong when the highly conducting central channel, which responds to magnetic perturbations, is narrow, as in the present example. The external magnetic field, and proximity of the conducting guide at R_c are seen to be stabilizing.

To further illustrate the dependence of stability properties on the fractional current neutralization f_m, plots of (a) the growth rate Ω_i and (b) the real frequency Ω_r, versus $\omega\tau_d$, are shown in Fig. 4,

for $\omega_c = R_b/R_c = 0$ and various values of f_m. It is evident that as the fractional current neutralization increases to unity, the growth rate increases rapidly (for reasons discussed previously), while the real oscillation frequency decreases (because the magnetic restoring force is being canceled out). We note also that in all cases the maximum growth rate Ω_i occurs for $\omega\tau_d < 1$, which is the reason we are mainly interested in this regime. For $f_m << 1$, the instability is driven mainly by a phase lag between the oscillation of the beam and that of the magnetic restoring force, and the growth rate peaks for $\omega\tau_d$ only slightly less then unity, but for $f_m \geq 0.4$, instability is driven mainly by the simple repulsion of the beam current and the equilibrium current, and the growth rate is remarkably flat for $\omega\tau_d \leq 0.3$, actually reaching its maximum at $\omega\tau_d = 0$.

In Fig. 5, Ω_i and Ω_r are plotted against ω_c, for $f_m = 0$, $R_b/R_c = 0.4$, and several small values of $\omega\tau_d$. We note that increasing the guide B_{oz} field (i.e. ω_c) reduces the growth rate Ω_i considerably (but never to zero). As shown in Fig. 3, as well, the growth rate Ω_i increases with $\omega\tau_d$ in this range, but Ω_r is very insensitive to $\omega\tau_d$.

The influence of the conducting guide at R_c illustrated in Fig. 6, where Ω_i and Ω_r are plotted against ω_c for $f_m = 0$, $\omega\tau_d = 0.5$, and several values of the parameter R_b/R_c. As shown, the growth rate Ω_i falls rapidly to zero, while the oscillation frequency increases, as R_b/R_c increases to unity. The reason for both effects is, of course, the increasing stiffness of the magnetic field trapped between R_b/R_c.

In Fig. 7, Ω_i and Ω_r are plotted against ω_c for a fully current neutralized case, $f_m = 1$, with $R_b/R_c = 0.4$ and $\omega\tau_d = 0.5$. The growth rate, due to repulsion between the beam and the opposite plasma current is very strong for $\omega_c < \omega_{pb}\beta_b$, but falls off when $\omega_c \geq \omega_{pb}\beta_b$. For $f_m = 1$, $\omega_\beta \to 0$ and the beam is essentially confined only by the B_{oz} external field, hence the linear dependence of Ω_r on ω_c for $\omega_c \leq \omega_{pb}\beta_b$, as well as the strong stabilizing effect of increasing ω_c above $\omega_{pb}\beta_b$.

We summarize this section by noting that resistive hose instability can be driven either by a phase lag in the restoring force due to non-zero $\omega\tau_d$ or by the presence of a plasma return current; thus increasing f_m is destabilizing. Increasing the applied field ω_c reduces the growth rate, but never to zero. Proximity of the conducting guide, i.e. $R_b/R_c \to 1$, also exerts a strong stabilizing influence, but the growth rate remains positive until $R_b/R_c = 1$. These general features of the behavior should apply to a beam with diffuse profile as well as to the uniform beam discussed in this section. Additional effects of great interest occur in a diffuse beam, due to mixing of electrons with different resonant frequencies. These effects have been discussed by Lee within the context of his multiple-component rigid beam model,[3] and will be investigated further in subsequent papers, using the formal framework developed in this paper.

V. Conclusions

In this paper we have formulated a Vlasov-Maxwell theory of the resistive hose instability in an infinitely long relativisitc electron beam propagating parallel to a uniform applied axial magnetic field. A dense, resistive background plasma provides space charge neutralization. The equilibrium configuration and basic assumptions were summarized in Sec. II. A formal eigenvalue equation (36) was obtained in Sec. III A, and was reduced to an ordinary differential equation (47) in the cold fluid limit in Sec. III B, and in an approximate treatment of the special case of a square beam density profile in Sec. III C. Using a variational technique, an approximate dispersion relation was obtained in Sec. III D for arbitrary beam density profile, Eqs. (64) and (67). The dispersion relation was evaluated explicitly, in closed form, for either a Bennett profile or a square profile, including the effects of fractional current neutralization, the applied field, and (in the latter case) a conducting outer wall. Stability properties were illustrated and discussed in Sec. IV, for a square profile over a broad range of system parameters. It was found that the applied magnetic field and proximity to the conducting guide reduce the growth rate of the resistive hose instability, whereas even a small amount of current neutralization is strongly destabilizing, particularly at low frequencies.

Acknowledgements

The authors are grateful for comments by and discussions with Dr. William Sharp.

References

1. W. H. Bennett, Phys. Rev. 45, 890 (1934); D. A. Hammer and N. Rostoker, Phys. Fluids 13, 183 (1970); R. C. Davidson, "Theory of Non-Neutral Plasmas", Benjamin, Reading, Mass., 1974; R. C. Davidson and H. S. Uhm, Phys. Fluids 22, 1375 (1979).
2. M. N. Rosenbluth, Phys. Fluids 3, 932 (1960).
3. E. P. Lee, Phys. Fluids 21, 1327 (1978).
4. S. Weinberg, J. Math. Phys. 5, 1371 (1964); 8, 614 (1967).
5. R. Lee and M. Lampe, Phys. Rev. Lett. 31, 1390 (1973).
6. H. S. Uhm and R. C. Davidson, Phys. Fluids 21, 265 (1978).
7. E. J. Lauer, R. J. Briggs, T. J. Fessendon, R. E. Hester, and E. P. Lee, Phys. Fluids 21, 1344 (1978).
8. C. A. Kapetanakos, Appl. Phys. Lett. 25, 481 (1974).
9. E. P. Lee, UCID-16268 , Lawrence Livermore Laboratory (unpublished).
10. R. C. Davidson and H. S. Uhm, Phys. Fluids 21, 60 (1978).

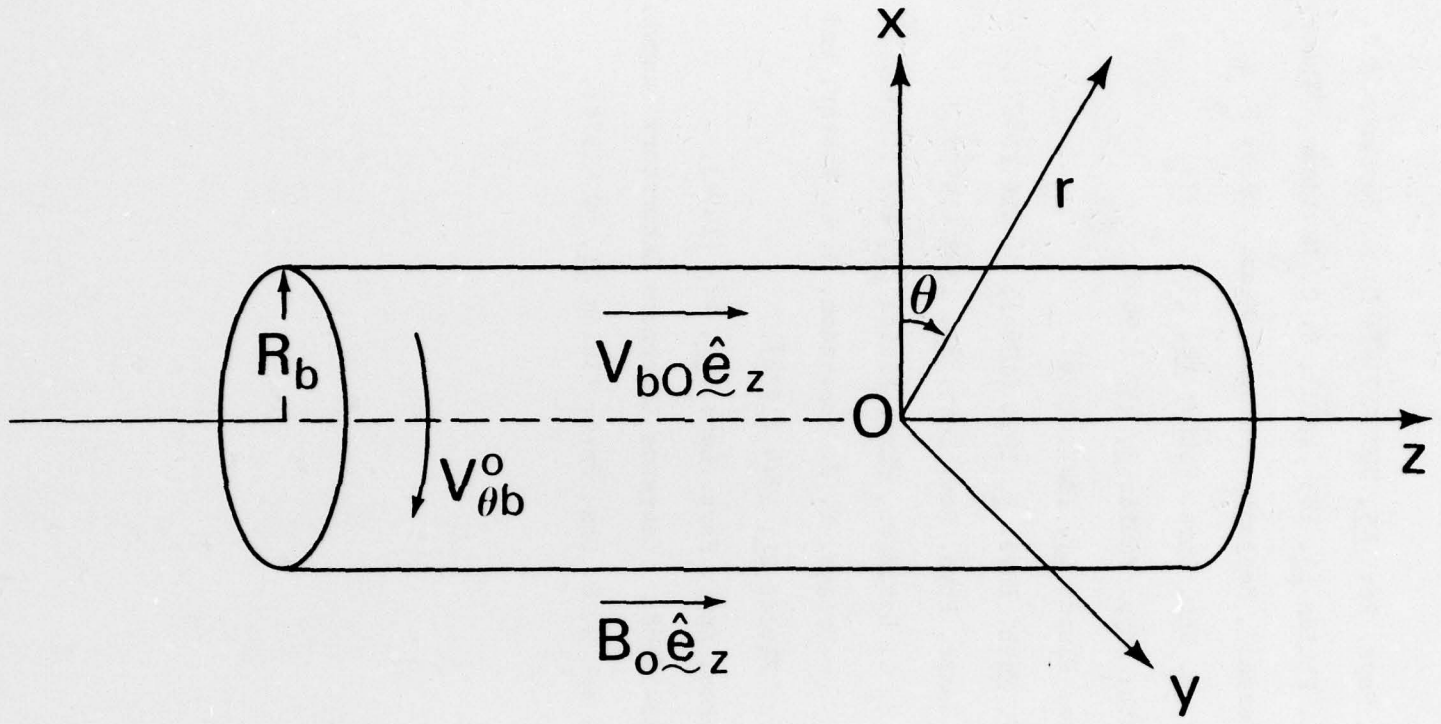

Fig. 1 — Equilibrium configuration and coordinate system

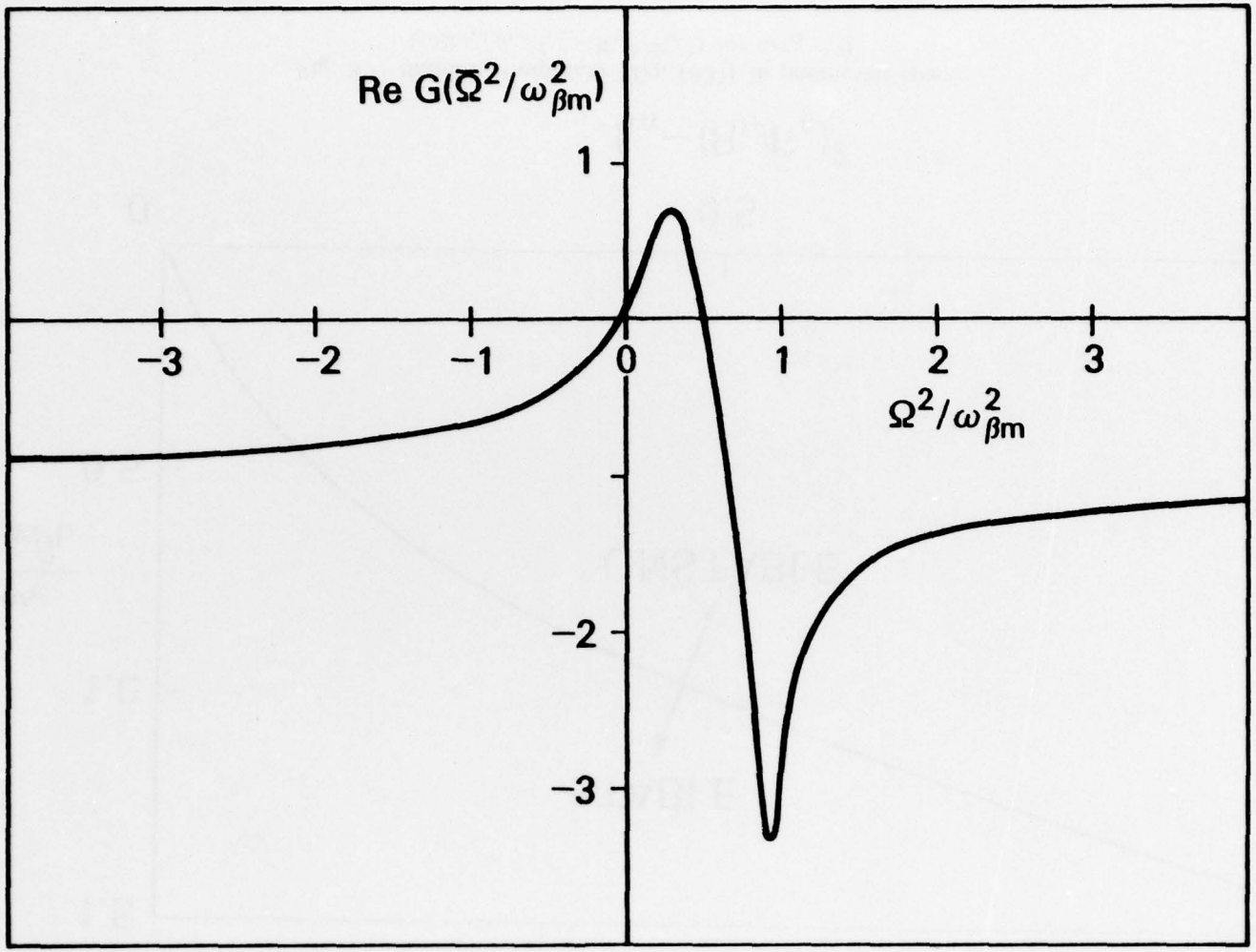

Fig. 2 — The function $G(\bar{\Omega}^2/\omega_{\beta m}{}^2)$ that appears in Eqs. (76)

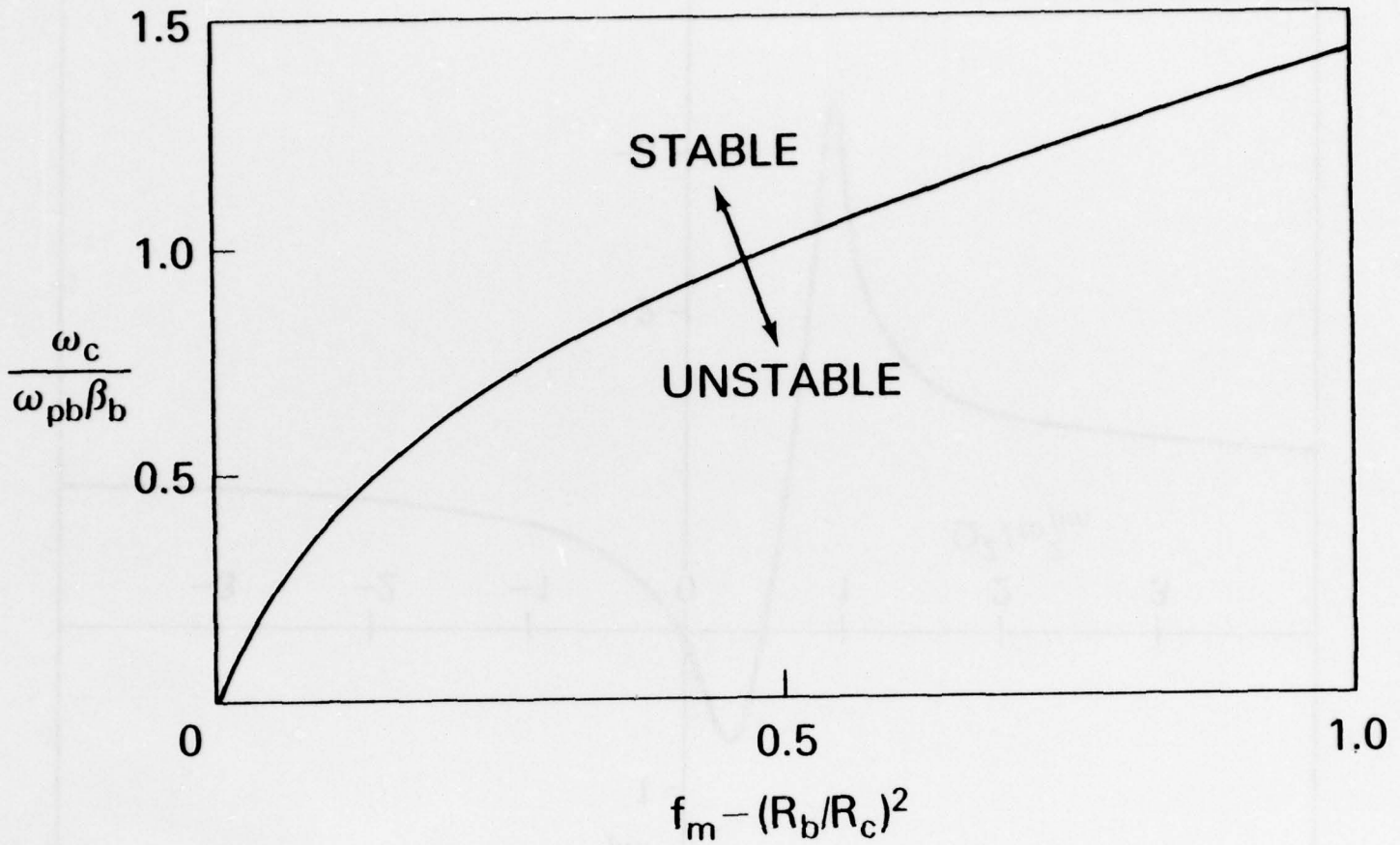

Fig. 3 — Stability boundary [Eq. (83)] in parameter space $(\omega/\omega_{pb}\beta_b, f_m - R_b^2/R_c^2)$ for $\omega\tau_d = 0$

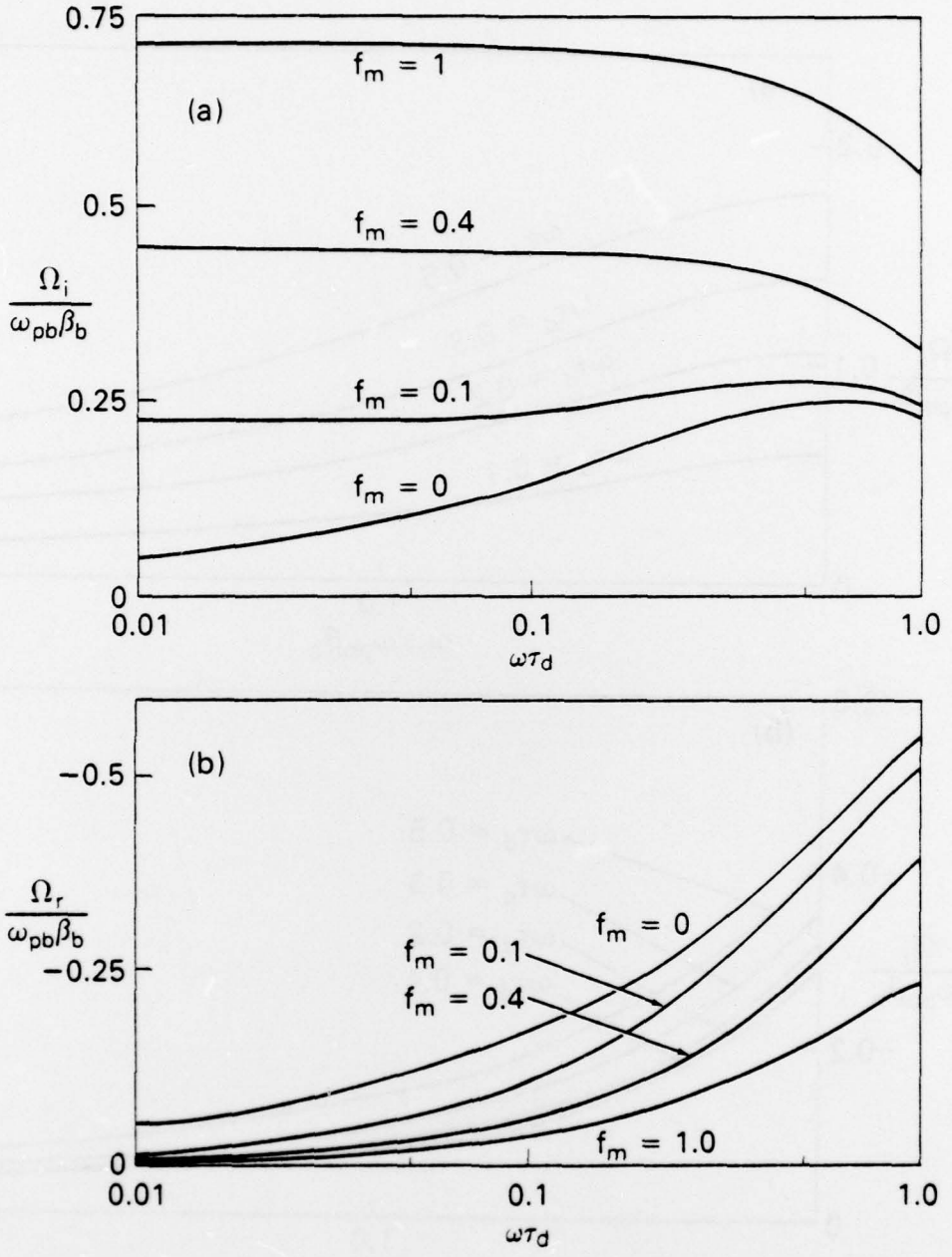

Fig. 4 — Plots of normalized (a) growth rate and (b) real Doppler-shifted frequency versus $\omega\tau_d$ for $\omega_c/\omega_{pb}\beta_b = 0$, $R_b/R_c = 0$ and values of f_m

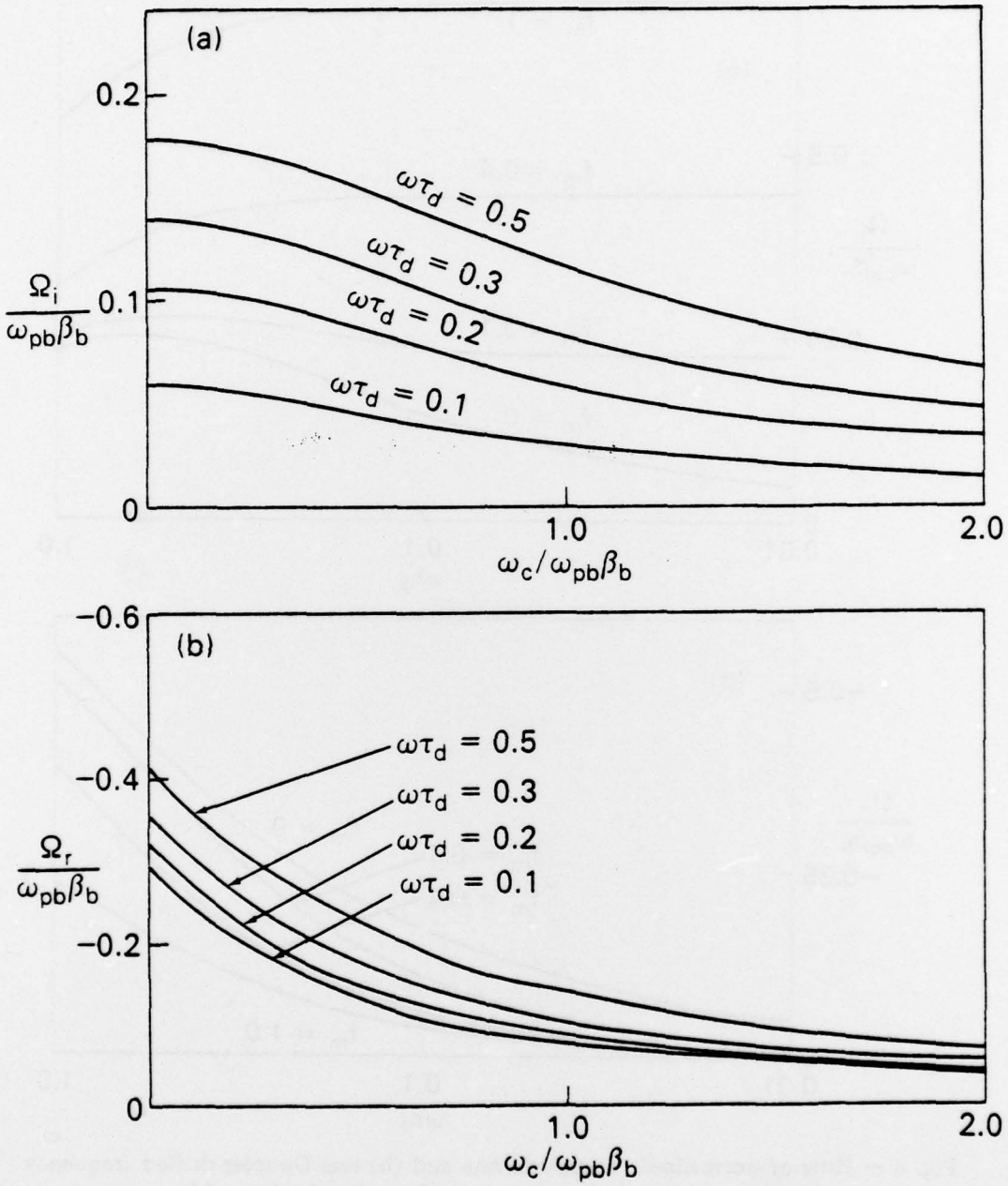

Fig. 5 — Plots of normalized (a) growth rate and (b) real oscillation frequency versus $\omega_c/\omega_{pb}\beta_b$ for $f_m = 0$, $R_b/R_c = 0.4$ and several values of $\omega\tau_d$

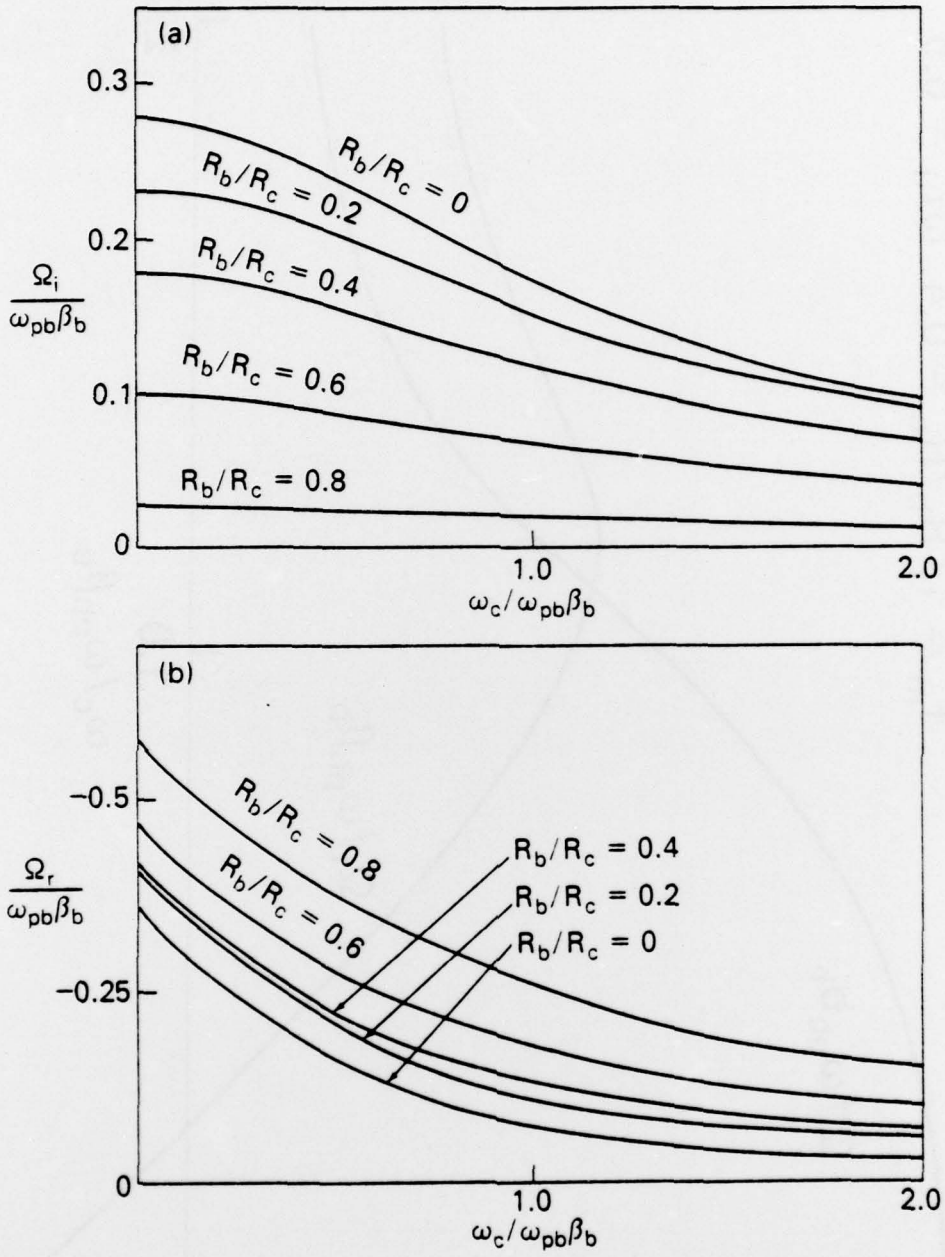

Fig. 6 — Plots of normalized (a) growth rate and (b) real oscillation frequency versus $\omega_c/\omega_{pb}\beta_b$ for $f_m = 0$, $\omega\tau_d = 0.5$ and several values of R_b/R_c

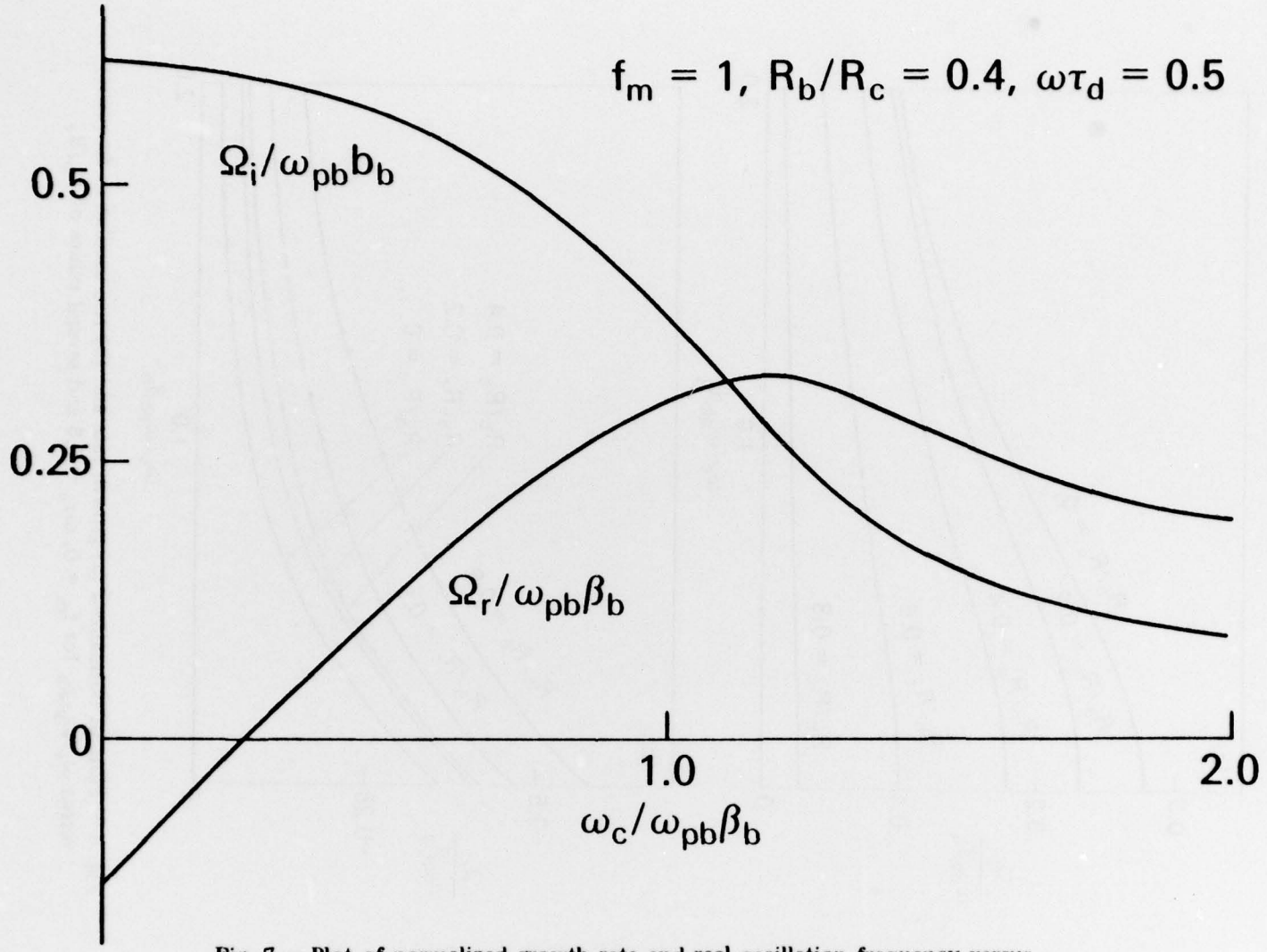

Fig. 7 — Plot of normalized growth rate and real oscillation frequency versus $\omega_c/\omega_{pb}\beta_b$ for $f_m = 1$, $R_b/R_c = 0.4$ and $\omega\tau_d = 0.5$